

Solvent Exchange Method: A Novel Microencapsulation Technique Using Dual Microdispensers

Yoon Yeo,¹ Alvin U. Chen,² Osman A. Basaran,² and Kinam Park^{1,3}

Received March 11, 2004; accepted April 5, 2004

Purpose. A new microencapsulation method called the "solvent exchange method" was developed using a dual microdispenser system. The objective of this research is to demonstrate the new method and understand how the microcapsule size is controlled by different instrumental parameters.

Methods. The solvent exchange method was carried out using a dual microdispenser system consisting of two ink-jet nozzles. Reservoir-type microcapsules were generated by collision of microdrops of an aqueous and a polymer solution and subsequent formation of polymer films at the interface between the two solutions. The prepared microcapsules were characterized by microscopic methods.

Results. The ink-jet nozzles produced drops of different sizes with high accuracy according to orifice size of a nozzle, flow rate of the jetted solutions, and forcing frequency of the piezoelectric transducers. In an individual microcapsule, an aqueous core was surrounded by a thin polymer membrane; thus, the size of the collected microcapsules was equivalent to that of single drops.

Conclusions. The solvent exchange method based on a dual microdispenser system produces reservoir-type microcapsules in a homogeneous and predictable manner. Given the unique geometry of the microcapsules and mildness of the encapsulation process, this method is expected to provide a useful alternative to existing techniques in protein microencapsulation.

KEY WORDS: dual microdispenser system; ink-jet technology; microencapsulation; protein delivery; solvent exchange.

INTRODUCTION

Microencapsulation is one of the most popular methods to produce controlled release parenteral dosage forms. In particular, microparticles made of biodegradable polymers, such as poly(lactic-co-glycolic acid) (PLGA), have extensively been investigated for delivery of various bioactive molecules (1–5). A number of microencapsulation methods have been developed to such a level that one can choose a proper method depending on the physicochemical properties of the drug and the polymer to be used (3,4,6–11). Such technological advances in the past decades have led to successful development of several commercial products (3,4,12–15). The double emulsion-solvent evaporation/extraction methods have widely been used in microencapsulation of water-soluble drugs.

One of the weaknesses of the existing methods, however, is their limitations in microencapsulation of bioactive pro-

teins, which are among the most attractive candidates for controlled release (5,16,17): Incomplete release of a protein and protein denaturation during preparation and release periods have often been found to be major problems (5,6,16–18). Possible causes for such problems include extensive exposure of proteins to the water/organic solvent (w/o) interface generated during emulsification (19–28), direct exposure of proteins to hydrophobic organic solvents (29,30), and physical stresses due to, for example, shear stress or elevated temperature (20,25,26,31). Acidic microenvironments or hydrophobic polymer surfaces, to which encapsulated proteins are likely to be exposed during the release stage, can also contribute to their denaturation (23,32,33). Another limitation is the use of chlorinated solvents such as methylene chloride, which could be a concern for environmental and human safety reasons (34); hence, there have been many attempts to replace this solvent with more benign organic solvents (19,20,35–42).

In an effort to alleviate some of these limitations, we have developed the solvent exchange method as a potential alternative to the existing techniques. The method was implemented using two ink-jet nozzles that continuously produce two streams of liquid drops. Collision of the two drops, arranged by precise manipulation of location of the two nozzles, leads to reservoir-type microcapsule formation. The objective of the current work is to demonstrate the solvent exchange method and understand instrumental parameters that affect the microcapsule size.

PRINCIPLES OF THE SOLVENT EXCHANGE METHOD

The solvent exchange method is based on a phenomenon that a solid polymer film forms at the interface between an aqueous solution and a solution of a water-insoluble polymer upon their contact. Figure 1A shows a polymer film forming on a surface of water. A drop of polymer solution was placed on the layer of water using a pipette. The last frame of the sequence shows lifting of the polymer film formed on the water surface. To examine the formation of a polymer film at the air–water interface using various solvents more easily, 0.5% agarose gel was used in lieu of water. The agarose gel provides an immobile aqueous platform, which facilitates evaluation of the films formed on its surface. Spreading of a solvent drop is clearly seen in the third frame of Fig. 1B. The last frame of Fig. 1B shows lifting of a thin film formed on the agarose gel surface. The main idea of this method is that one can produce reservoir-type microcapsules, consisting of a single aqueous core surrounded by a thin biodegradable polymer membrane, by replacing the water or the agarose gel layer with an aqueous drop.

Formation of a polymer film on the aqueous surface depends on spreading of the polymer solution on the aqueous surface and subsequent phase separation of the water-insoluble polymer. It was observed that the spreading of the polymer solution was mainly dictated by physical properties of the organic solvent. On the hydrogel surface, the polymer solution is exposed to two kinds of interfaces: an interface with air and an interface with a hydrogel. Because the hydrogel consists of >90% of water, the latter is virtually an interface with water. For favorable spreading of the polymer solution over the aqueous surface, the solvent is required to have a low interfacial tension with both water and air (i.e.,

¹ Departments of Pharmaceutics and Biomedical Engineering, Purdue University, West Lafayette, Indiana 47907, USA.

² Department of Chemical Engineering, Purdue University, West Lafayette, Indiana 47907, USA.

³ To whom correspondence should be addressed. (e-mail: kpark@purdue.edu)

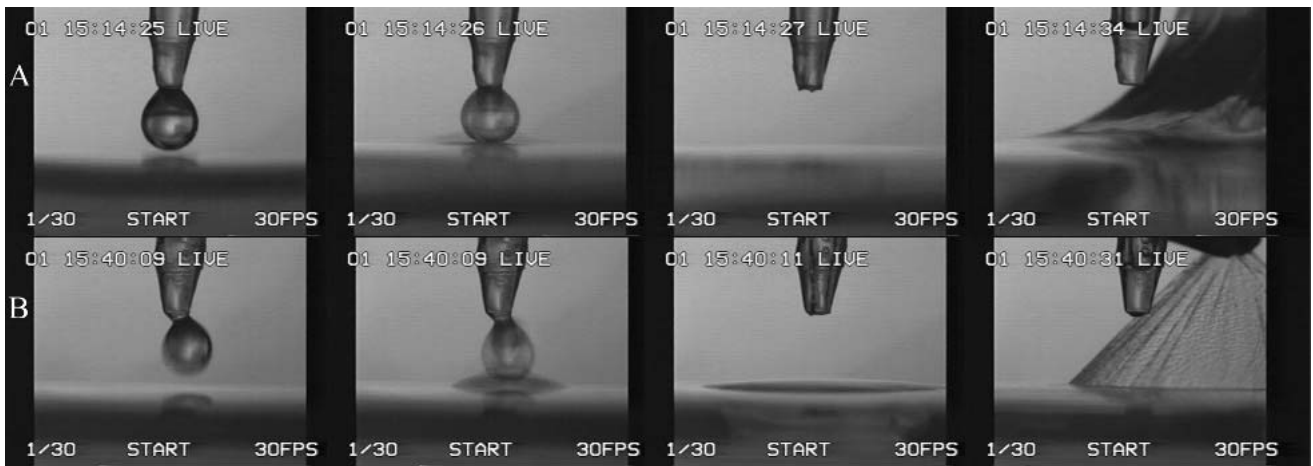


Fig. 1. Formation of a PLGA film at the water/air interface: A drop of 5% PLGA solution placed on a layer of (A) water and (B) 0.5% agarose gel spreads virtually instantaneously to form a solid film, viz. in less than 2 seconds for water and 10 seconds for the agarose gel.

surface tension) (43). Phase separation of the polymer film is a result of mass transfer between the organic solvent and water (i.e., solvent exchange) leading to decrease in the solubility of the polymer in the solvent. Organic solvents should be miscible with water to a certain degree in order to cause instant phase separation of the polymer film. Once a suitable solvent is determined, reservoir-type microcapsules can be formed by inducing the spreading and the phase separation to occur on the surface of an aqueous drop. Under the criteria described above, ethyl acetate was found to be one of the best solvents among those tested in our laboratory (44).

One way to encapsulate an aqueous drop by a polymer solution is to simultaneously produce drops of the aqueous and polymer solutions and to induce midair collision between

the two drops. An ink-jet nozzle controlled by a piezoelectric transducer was found to be suitable for our application and able to produce microdrops of a predictable size. In the present study, two ink-jet nozzles in which one produces aqueous drops and the other drops of a polymer solution, respectively, were aligned to allow collision of pairs of microdrops emerging from each nozzle, as described in Fig. 2. It is believed that the hydrodynamic fates of two drops upon collision are determined by the surface tensions of the liquids: The organic solvent preferentially deforms and spreads on the aqueous drop upon contact, whereas the aqueous drop, which has a relatively higher surface tension as compared to that of the organic solvent, tends to maintain its spherical shape. The solvent exchange process begins as soon as the two micro-

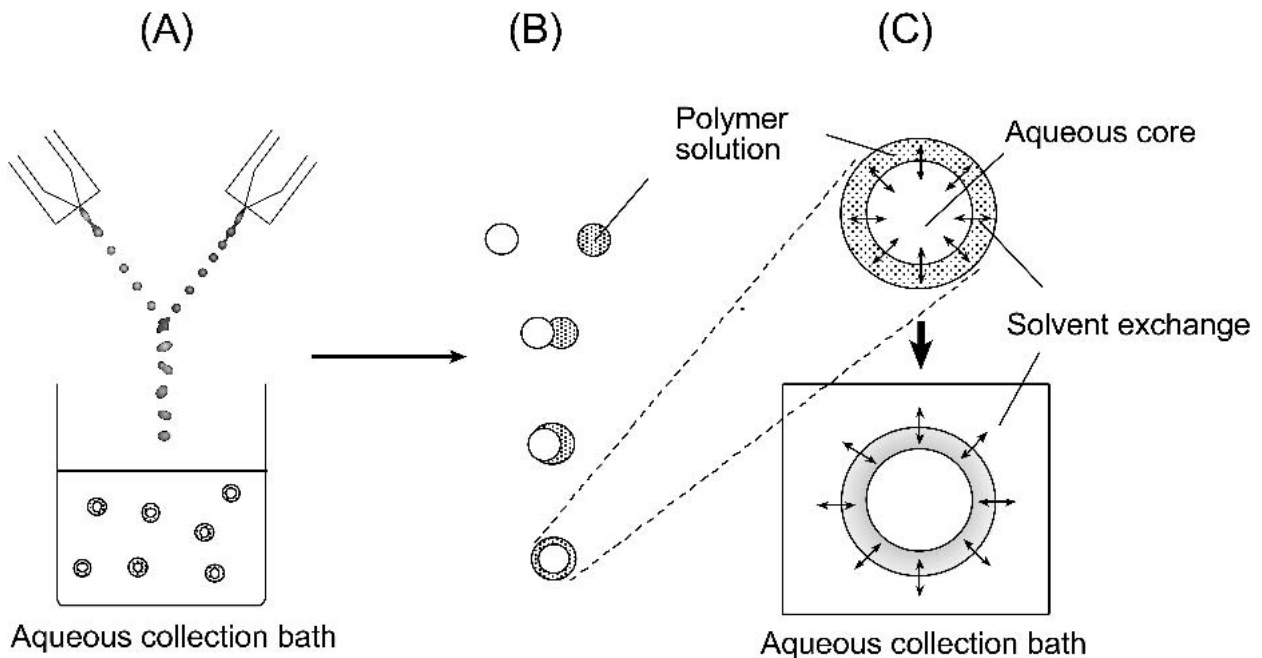


Fig. 2. Formation of microcapsules by the solvent exchange method using a dual microdispenser system. (A) One ink-jet nozzle generated aqueous microdrops and the other generated microdrops of a polymer solution. (B) The two ink-jet nozzles were aligned to cause midair collision between two microdrops. (C) Solvent exchange proceeded at the interface between two liquids to form a polymer layer on the aqueous drop. Microcapsules thus formed were collected in the aqueous bath. The left picture was drawn based on digital images obtained using stroboscopic illumination for clear presentation.

drops come in contact and is completed in the aqueous bath, where the compound drops are collected, as described in Fig. 2.

MATERIALS AND METHODS

Materials

Poly (lactic-co-glycolic acid) [PLGA; lactide to glycolide ratio (L/G) = 50/50, inherent viscosity = 0.59 dl/g] was obtained from Birmingham Polymers, Inc. (Birmingham, AL, USA) (lot: D01070). Polyvinyl alcohol (PVA; 98.0–98.8% hydrolyzed; MW ~195,000, no. 10851) was obtained from Fluka (Milwaukee, WI, USA). Ethyl acetate (EA, 4992-04), calcium chloride dehydrate (4106), and methylene chloride (4879) were obtained from Mallinckrodt Baker, Inc. (Phillipsburg, NJ, USA). Coomassie Brilliant Blue R-250 (161-0400) was purchased from Bio-Rad. Nile Red (N3013) (Hercules, CA, USA), Fluorescein isothiocyanate-dextran (FITC-dextran, MW ~42,000, FD-40S), and sodium alginate (A2033) were obtained from Sigma (St. Louis, MO, USA). Agarose (Seakem LE; lot: 61426) was obtained from FMC BioProducts (Rockland, ME, USA).

Preparation of Microparticles

Solvent Exchange Method Using a Dual Microdispenser Assembly

Figure 3 describes a dual microdispenser system that consists of two ink-jet nozzles. Microcapsules were produced as described previously (44). Briefly, a solution of 2% PLGA in ethyl acetate and an aqueous solution containing 0.2% sodium alginate were delivered into two different nozzles, respectively. Dyes were optionally added in each solution. Size of the nozzle orifice was the same for both nozzles: either 40 or 60 μm in diameter (MicroFab Technologies, Inc., Plano, TX, USA). The liquid streams were perturbed by a frequency generator (Hewlett-Packard model 33120A, Hewlett-Packard/Agilent, Palo Alto, CA, USA) to produce a series of uniform drops. Locations of two nozzles were precisely manipulated to cause collisions between the drops. The formed microcapsules were collected in a water bath containing 0.15 M calcium chloride. The microcapsules were collected using a centrifuge, washed with distilled water at least three times, and lyophilized for 24 h.

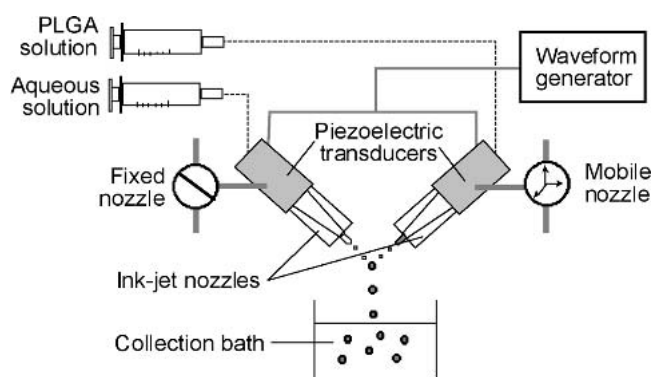


Fig. 3. Schematic description of a dual microdispenser system.

Double Emulsion-Solvent Evaporation Method

For comparison, microspheres were also produced using a double emulsion-solvent evaporation method described in the literature (45) with a slight modification. Fifty microliters of aqueous FITC-dextran solution (20%) was poured into 1 ml of methylene chloride containing 33% PLGA and 0.003% Nile Red. The solution was mixed for 1 min using a vortex mixer. The resulting w/o emulsion was poured under magnetic stirring into 2 ml of aqueous 1% PVA solution saturated with methylene chloride to form a water in organic solvent in water (w/o/w) double emulsion. The w/o/w emulsion was poured into 200 ml of water containing 0.1% PVA and continuously stirred for 3 h at room temperature until most of the methylene chloride evaporated, leaving solid microspheres. The microspheres were collected by centrifuge, washed with distilled water at least three times, and lyophilized for 24 h.

Morphological Characterization of Microparticles

Bright-Field Microscopy

Nascent microcapsules were observed using a bright-field microscope. Drops consisting of a suspension of microcapsules were placed on a glass cover slip and the microcapsules were observed with a Nikon Labophot 2 microscope (Japan). Sizes of the microcapsules were determined from the bright-field microscopic images. Reported values are averages of 30–50 microcapsules.

Confocal Laser Scanning Microscopy

The internal structure of the microparticles was imaged using an MRC-1024 Laser Scanning Confocal Imaging System (Bio-Rad) equipped with a krypton/argon laser and a Nikon Diaphot 300 inverted microscope. The collected microparticles were centrifuged and washed with distilled water prior to observation. All confocal fluorescence pictures were taken with a 20 \times objective and excitation at 488 nm and 568 nm. Green and red fluorescence images and a transmission image were obtained from separate channels.

Particle Size Control Using an Ink-Jet Nozzle

Distilled water was supplied to an ink-jet nozzle with an orifice of diameter d of 30 or 60 μm at flow rates Q ranging from 0.3 to 0.7 ml/min for $d = 30 \mu\text{m}$ and from 0.6 to 2.0 ml/min for $d = 60 \mu\text{m}$. The water stream was perturbed at different frequencies f to produce uniform drops. The drop sizes were determined from stroboscopic images. Apparently, the drops were highly homogeneous in size; thus, representative one was taken to determine the size generated under the specific condition.

RESULTS

Formation of Microcapsules by the Solvent Exchange Method

As shown in Fig. 4, the microcapsules prepared by the solvent exchange method appeared transparent when observed by a bright-field microscope indicating that the surrounding polymer layer was a thin membrane. The blue color

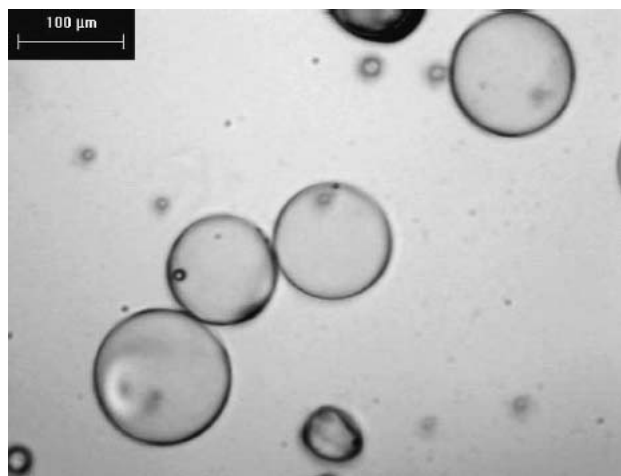


Fig. 4. Bright-field micrograph of mononuclear microcapsules produced by the solvent exchange method. Bar = 100 μm .

of the main spherical bodies of the microcapsules confirmed that encapsulated was the aqueous dye solution.

Microparticles produced by the solvent exchange method and those by the double emulsion-solvent evaporation method were compared with respect to their internal structures using confocal microscopy, as shown in Fig. 5. In both cases, the aqueous phase was labeled with FITC-dextran, and the polymer matrix or membrane was visualized by Nile Red, a lipophilic fluorescence dye, dissolved along with the polymer in the organic solvent. Figure 5 makes plain that the microcapsule produced by the solvent exchange method was composed of a single drop of the aqueous phase surrounded by a polymer membrane. In contrast, the microspheres produced by the double emulsion method consisted of multiple drops of the aqueous solution embedded within the polymer matrix.

Control of Drop Size Using an Ink-Jet Nozzle

When microdrops are produced from an ink-jet nozzle perturbed by a piezoelectric transducer, their diameters d_d depend on three variables: diameter d of the orifice, average velocity of the jetted solution V , and forcing frequency f . A liquid jet, assumed to be a cylinder of diameter d , would break into uniform drops of volume $\pi(d/2)^2\lambda$, where $\lambda = V/f$ is the wavelength of the imposed perturbation. The diameter d_d of the drops that are thereby produced can be obtained by equating the volume of the cylinders to that of the resulting spheres:

$$d_d = \left(\frac{3d^2V}{2f} \right)^{\frac{1}{3}} \quad (1)$$

Because V equals the volumetric flow rate Q in cm^3/min divided by the cross-sectional area of the orifice $\pi(d/2)^2$, Eq. 1 can be rewritten as:

$$d_d = \left(\frac{6Q}{\pi f} \right)^{\frac{1}{3}} \quad (2)$$

In Eq. 2, the diameter of the formed microdrops is a function of only Q and f , but the nozzle orifice diameter d is implicitly involved by constraining the range of values of Q as well as f , which breaks up a liquid stream into uniformly sized drops at a given flow rate Q . In other words, the drop size is primarily determined by orifice size of the ink-jet nozzle.

The smallest attainable size of drops is of primary interest in terms of utility of this method; therefore, it is necessary to define practical ranges of Q and f as well as the smallest size of drops that can be produced by a given nozzle. In the current study, nozzles with orifice diameters of 30 μm and 60 μm were used to produce water drops of uniform size at different Q s. At each value of Q , f was varied to find the maximum possible value that would produce the smallest drops.

The size of drops issued from the ink-jet nozzles, determined experimentally from the stroboscopic images, agreed well with the theoretical values calculated from Eq. 2. Figures 6 and 7 show that the drop size decreased with increasing frequency at a fixed flow rate. When the drop sizes were compared for different flow rates at a fixed frequency, the size increased with increasing flow rate for all values of frequency, as shown in Table I. When both flow rate and frequency were varied at the same time, however, it was not necessarily at the lowest flow rate that the smallest drop size resulted. The reason is that the maximum attainable frequency, defined as a frequency above which a liquid jet does not break up into homogeneous drops, increased with the flow rate. The maximum attainable frequency increased in proportion to the flow rate with a high linearity ($r^2 = 0.9993$ for the 30- μm orifice and 0.9991 for the 60- μm orifice) (Fig. 8). The smallest possible drop size that can be obtained at each flow rate was almost the same ($\sim 46 \mu\text{m}$) at all flow rates for the 30- μm nozzle (Table II). For the 60- μm nozzle, the increase in the flow rate increased the maximum attainable frequency further; hence, smaller drops were produced at higher flow rates.

Effects of Nozzle Parameters on Size of Microcapsules

The diameters of microcapsules were estimated using a bright-field microscope and compared with theoretical values and those of drops obtained from the stroboscopic images. As

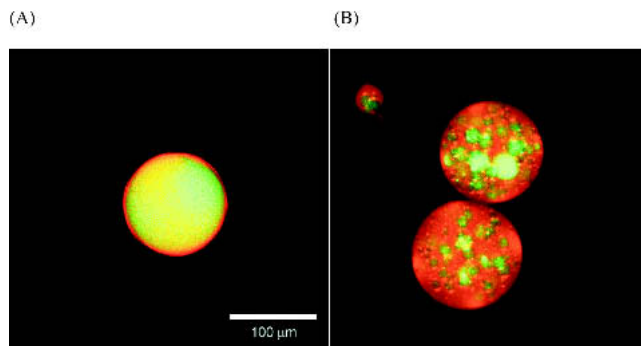


Fig. 5. Confocal fluorescence microscopic images of microspheres produced by (A) the solvent exchange method and by (B) the double emulsion solvent evaporation method. The images were produced by projecting multiple layers of pictures on top of each other. The PLGA phase appears red due to the presence of Nile Red, and the aqueous phase appears green due to the presence of FITC-dextran.

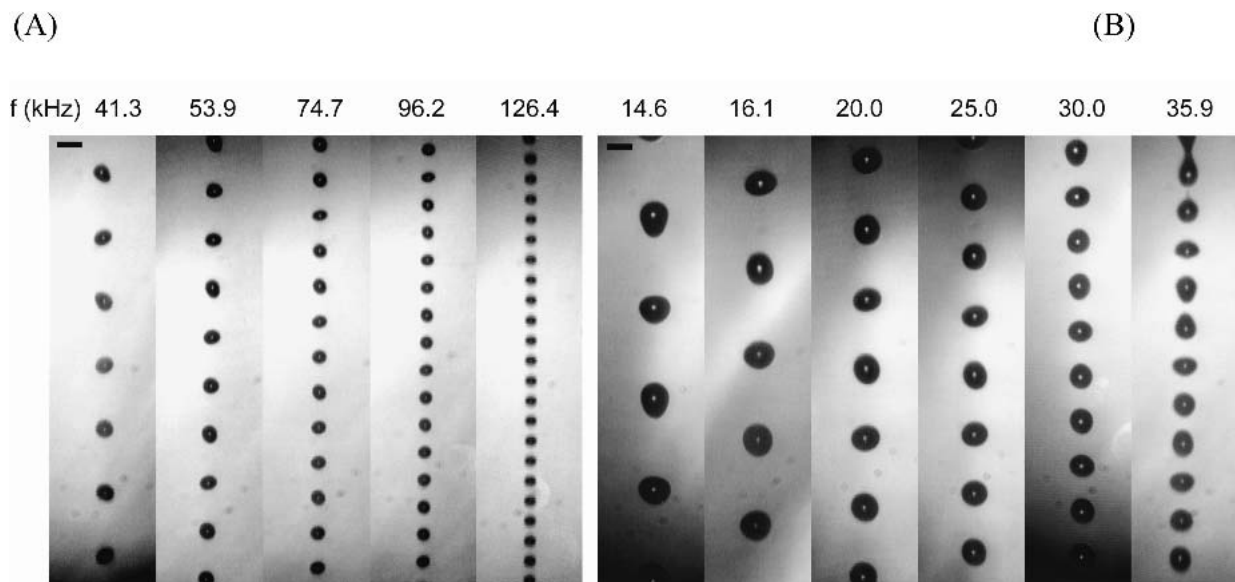


Fig. 6. Aqueous drops produced by ink-jet nozzles driven in a continuous mode using a nozzle of (A) 30- μm orifice and (B) 60- μm orifice under different frequencies at a fixed flow rate (0.5 ml/min for the 30- μm orifice and 1.0 ml/min for the 60- μm orifice). Pictures were taken using a strobe and a video camera so that the drops in each image were actually superposition of many successive drops. Scale bar = 100 μm .

described above, the size of single drops issued from each nozzle is determined by flow rate (Q) and forcing frequency (f), which are primarily limited by the nozzle orifice. The size of a merged drop resulting from the union of two spherical drops would be calculated by:

$$r_w^3 + r_o^3 = r_m^3 \quad (3)$$

where r_w , r_o , and r_m are the radii of microdrops of the aqueous solution, the polymer solution, and the merged drops, respectively. If the sizes of two microdrops are the same (i.e.,

$r_w = r_o$) and there is no loss of material upon their collision, r_m would be $1.26r_w$, which means that the layer of polymer solution would be as thick as 26% of the radius of a single drop. It is also expected that the size distribution of the microcapsules will be as homogeneous as that of single drops. The sizes measured from the stroboscopic pictures satisfied these expectations for both single and merged drops (Table III and Fig. 9). Majority of the microcapsules collected in the bath were similar in size (defined as “unit size”) when observed by a microscope. On the other hand, it is interesting to notice that the unit size of collected microcapsules was

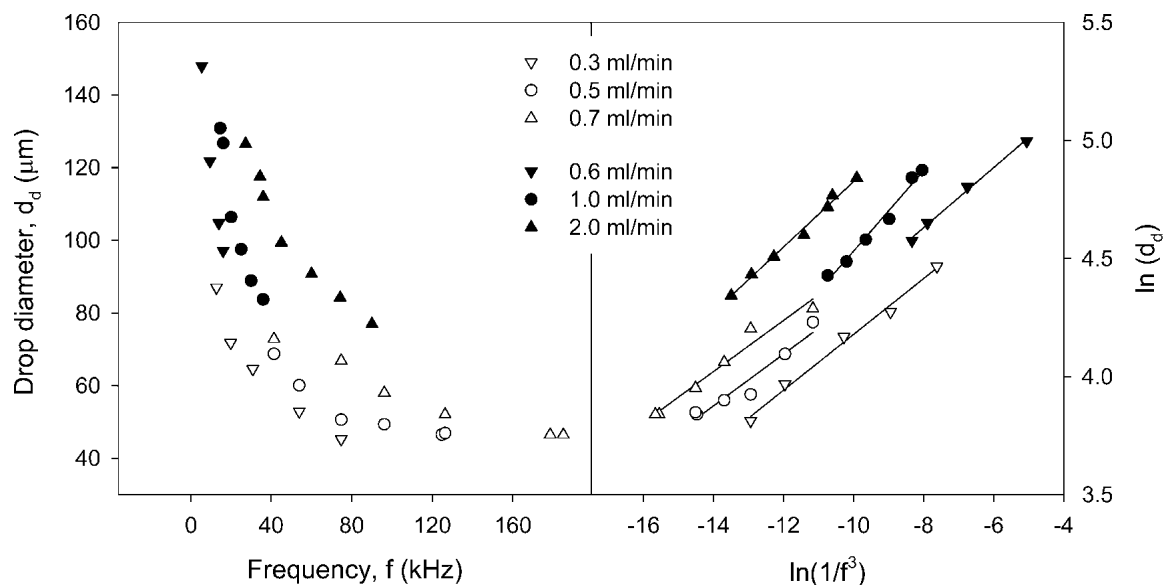


Fig. 7. Relationship between drop diameters and forcing frequencies. Open symbols represent results obtained with the 30- μm orifice and solid symbols represent those obtained with the 60- μm orifice. The graph in the right is alternative representation of the left showing that the relationship is in good agreement with Eq. 2.

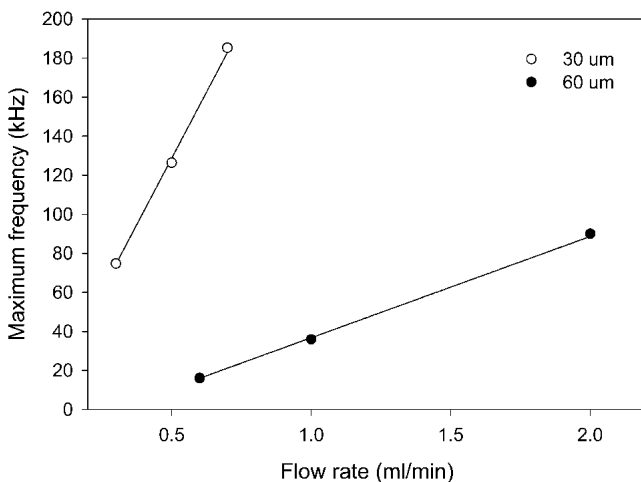
Table I. Dependence of Drop Diameter on the Flow Rate at a Fixed Forcing Frequency for a 30 μm -Orifice Nozzle

Frequency, <i>f</i> (kHz)	Flow rate, <i>Q</i> (ml/min)	Drop diameter (μm)
41.3	0.50	68.7
41.3	0.70	72.8
53.9	0.30	52.9
53.9	0.50	60.1
74.7	0.30	45.3
74.7	0.50	50.6
74.7	0.70	66.9
96.2	0.50	49.4
96.2	0.70	58.0
126.4	0.50	46.9
126.4	0.70	52.1

equivalent to that of single drops emerging from an ink-jet nozzle (Table III), and the polymer layer existed only as a thin membrane. According to scanning electron microscope observation (data not shown), thickness of the membrane was 1–2 μm on the average. The unit size displayed dependence on the frequency applied to the liquid jet ($p < 0.05$, Table IV and Fig. 10) as well as the orifice diameter. However, the collected group of microcapsules occasionally included micro-particles of unexpected sizes. Our preliminary study using confocal microscopy suggests that the small satellites are made of the polymer phase. It is possible that the shear stress caused by stirring of the collection bath might have separated parts of the polymer layer that was originally associated with the aqueous core. It is also possible that the satellites originated either from the break-up of the polymer solution jet or due to the collision between the polymer drop and the aqueous drop.

DISCUSSION

The solvent exchange method was implemented to produce microcapsules using a dual microdispenser system. Microscopic observations supported formation of reservoir-type microcapsules. In particular, confocal microscopy utilizing

**Fig. 8.** Relationship between the maximum frequency and the flow rate.**Table II.** The Smallest Drop Sizes at Different Flow Rates

Nozzle orifice (μm)	Flow rate, <i>Q</i> (ml/min)	Maximum frequency, <i>f</i> (kHz)	Drop diameter (μm)
30	0.3	74.7	45.3
30	0.5	126.4	46.9
30	0.7	185.2	46.5
60	0.6	16.1	97.1
60	1.0	35.9	83.7
60	2.0	90.0	77.0

phase-specific fluorescence dyes proved to be useful in visualization of the internal structure of the microcapsule. From the confocal micrographs, it was clear that contact between the aqueous and the polymer solutions was minimal and limited to the surface of the aqueous drop in the microcapsules produced by the solvent exchange method, as opposed to those produced by the double emulsion method. It is believed that this limited amount of contact will be especially advantageous for encapsulation of protein drugs, which can easily undergo irreversible aggregation at the w/o interface (19–28,46–49).

Another advantage of the dual microdispenser system is that it provides a good opportunity to control the particle size distribution. An ink-jet nozzle generates uniform drops of a desirable size. For this reason, the ink-jet technology has recently received considerable attention in the microencapsulation area. The technology has been used for precise control over the size distribution of dispersed phases in the emulsion-solvent evaporation/extraction method (50,51). Recently, ink-jet technology has been used to produce paclitaxel-loaded PLGA microspheres of a narrow size distribution and a controllable diameter (52).

In the solvent exchange method, the size of drops emerging from each ink-jet nozzle is a major determinant of the microcapsule size as well as the polymer membrane thickness. In order to understand instrumental parameters that are relevant to the microcapsule size and to determine the minimal drop size that can be produced under given conditions, the effects of orifice diameter, flow rate of the liquid, and forcing frequency imposed on the liquid jet on the drop size were investigated. The drop size was primarily determined by the

Table III. Comparison of Unit Sizes of Collected Microcapsules Produced by Different Nozzle Orifices

	(A)	(B)
Conditions		
Nozzle diameter (<i>d</i>)	60 μm	40 μm
Flow rate (<i>Q</i>)	0.6 ml/min	0.32 ml/min
Frequency (<i>f</i>)	10.6 kHz	10.9 kHz
Single drop		
Theoretical	121.7 μm	97.8 μm
Observed (strobe image)	115.4 μm	93.0 μm
Merged drop		
Theoretical	145.4 μm	123.2 μm
Observed (strobe image)	143.0 μm	117.3 μm
Microcapsules		
Observed (microscopic image)	115.6 \pm 5.3 μm	93.8 \pm 3.1 μm

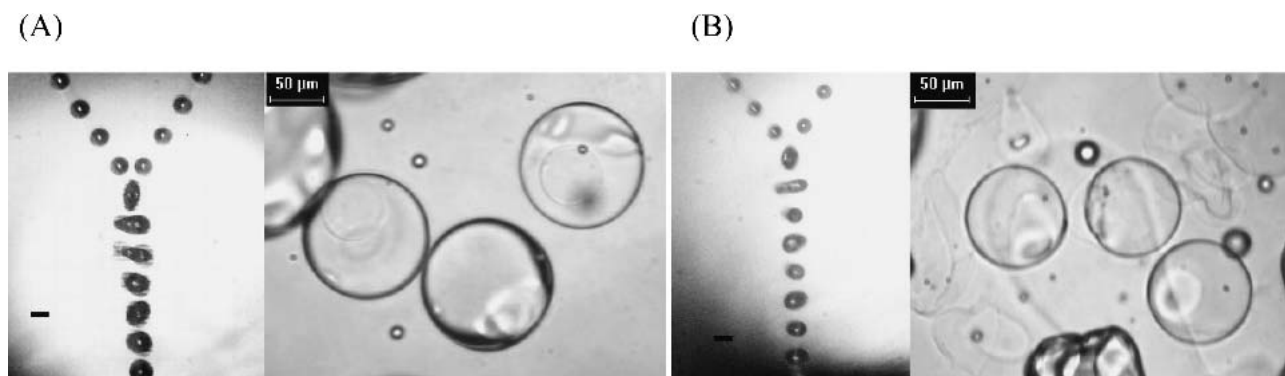


Fig. 9. Stroboscopic images of microcapsule formation and bright-field microscope images of microcapsules formed under the conditions specified in Table III.

orifice diameter. For a fixed nozzle orifice size, the drop size decreased with increasing (decreasing) frequency (flow rate) when the flow rate (frequency) was held constant. When both parameters were varied, the lower limit of drop size was determined by the maximum attainable frequency. That is, in order to produce small microdrops, despite its adverse effect on the small size, the flow rate needs to be increased to afford a high frequency. On the other hand, high flow rates can cause problems such as splashing of drops upon collision because of their higher inertia. Because this can result in loss of encapsulated drugs, it is not necessarily desirable to increase the flow rate. Instead, it may be more realistic to decide first on a practical flow rate and then to increase the frequency as much as possible to produce the smallest drops.

The smallest possible size of single drops was approximately 130% to 150% of the nozzle orifice diameter. For example, the smallest sizes were 46 μm and 77 μm for the 30- μm orifice and the 60- μm orifice, respectively. To produce microdrops as small as 10–40 μm , it will be necessary to reduce the orifice size down to 5–25 μm . Alternatively, the drop size can be reduced by running the ink-jet nozzle in a special mode called the drop-on-demand, in which the drop diameter can approximately equal the orifice diameter (53). Furthermore, it was recently found that drops having diameters of 1/2 to 1/3 of the orifice diameter could be produced by applying a special waveform (53). Using the waveform modulation, it was possible to produce drops of 15 μm in diameter from a 40- μm orifice nozzle (53).

The sizes of single and merged drops measured from the stroboscopic images taken during the midair collision coincided with theoretical values. This indicated that there was no

loss in volume when two drops collided in air. However, thickness of the polymer membrane of microcapsules collected in the water bath was much smaller than what was expected from Eq. 3. First, this can be attributed to the volume loss due to the removal of the solvent from the polymer phase. It is likely that the polymer layer shrank as the solvent that constituted 98% of the polymer phase was extracted by the solvent exchange with the aqueous phases. Given that the solid polymer occupied only 2% of the entire volume, it may be natural that the polymer layer ended up being a thin membrane and the size of the microcapsule was close to that of a single drop. On the other hand, considering the existence of the satellites, it is also possible that portions of the polymer layer separated during stirring of the bath and, thus, resulted in reduction of the membrane thickness.

From the mild nature of the encapsulation process and the unique geometry of the microcapsules, it is expected that this method will provide several advantages over contemporary methods, especially in encapsulation of proteins or peptides. First, the process does not include potentially damaging conditions such as an emulsification step, which often exerts unfavorable influences on the stability of encapsulated drugs by exposing them to the w/o interface and excessive physical stress. Second, in the mononuclear microcapsules, undesirable interactions between protein and organic solvent or polymer matrix are limited only to the interface at the surface of the core. However, whether these potential advantages will be reflected through enhanced release profiles and stability of the encapsulated proteins remains to be seen. Third, the organic solvent for polymers can be chosen with more flexibility than in conventional methods; hence, toxicity concerns over

Table IV. Dependence of Unit Sizes of Microcapsules on Forcing Frequency

	Nozzle diameter (d)		
	60 μm	60 μm	60 μm
Conditions			
Flow rate (Q)	0.7 ml/min	0.7 ml/min	0.7 ml/min
Frequency (f)	9.7 kHz	13.1 kHz	15.1 kHz
Single drop			
Theoretical	131.9 μm	119.4 μm	113.8 μm
Observed (strobe image)	122.7 μm	110.8 μm	108.1 μm
Microcapsules			
Observed (microscopic image)	119.0 \pm 6.4 μm	114.9 \pm 6.4 μm	106.8 \pm 7.6 μm

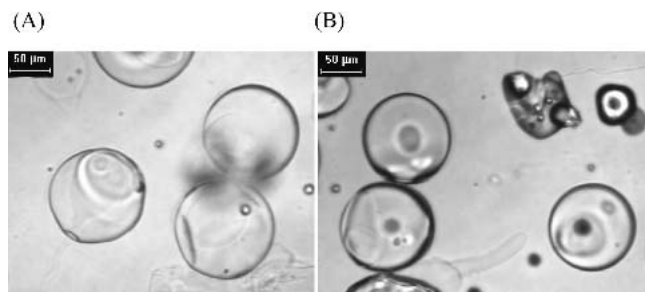


Fig. 10. Bright-field microscope images of microcapsules formed under the conditions specified in Table IV. Microcapsules were produced at (A) 9.7 kHz and (B) 15.1 kHz.

residual solvents, in particular methylene chloride, can be avoided. Fourth, the use of ink-jet nozzles allows for a precise control over the particle size. Fifth, scale-up of the microencapsulation process can easily be achieved by simply increasing the number of pairs of nozzles; thus, the quality of the microcapsules would not be affected by the scale-up process.

CONCLUSIONS

A new microencapsulation method called the solvent exchange method was developed based on instantaneous formation of a polymer film at the interface between an aqueous solution and an organic polymer solution upon their contact. The solvent exchange method was implemented using a microdispenser system consisting of two ink-jet nozzles, which allows collision of drops of two solutions in air. The solvent exchange method produced reservoir-type mononuclear microcapsules of hydrophilic cores surrounded by polymer membranes. Particle size could readily be controlled by instrumental variables related to the nozzle operation. Because the polymer layer became a thin membrane after completion of solvent exchange, an aqueous core was the major determinant of the microcapsule size.

ACKNOWLEDGMENTS

This study was supported in part by National Institute of Health through grant GM67044, Samyang Corporation, Purdue Research Foundation, NSF Industry/University Center for Pharmaceutical Processing Research, and the Basic Energy Sciences Program of the U.S. DOE.

REFERENCES

1. L. M. Sanders, J. S. Kent, G. I. McRae, B. H. Vickery, T. R. Tice, and D. H. Lewis. Controlled release of LHRH analogue from PLGA microspheres. *J. Pharm. Sci.* **73**:1294–1297 (1984).
2. M. S. Hora, R. K. Rana, J. H. Nunberg, T. R. Tice, R. M. Gilley, and M. E. Hudson. Release of human serum albumin from PLGA microspheres. *Pharm. Res.* **7**:1190–1194 (1990).
3. Y. Ogawa, M. Yamamoto, S. Takada, H. Okada, and T. Shimamoto. Controlled-release of leuprolide acetate from PLA or PLGA microcapsules: influence of molecular weight and copolymer ratio of polymer. *Chem. Pharm. Bull.* **36**:1502–1507 (1988).
4. J. L. Cleland, O. L. Johnson, S. Putney, and A. J. S. Jones. Recombinant human growth hormone poly(lactic-co-glycolic acid) microsphere formulation development. *Adv. Drug Delivery Rev.* **28**:71–84 (1997).
5. S. P. Schwendeman. Recent advances in the stabilization of proteins encapsulated in injectable PLGA delivery systems. *Crit. Rev. Ther. Drug Carrier Syst.* **19**:73–98 (2002).

6. Y. Yeo, N. Baek, and K. Park. Microencapsulation methods for delivery of protein drugs. *Biotechnol. Bioprocess Eng.* **6**:213–230 (2001).
7. S. Stassen, N. Nihant, V. Martin, C. Grandfils, R. Jerome, and R. Teyssie. Microencapsulation by coacervation of PLGA: 1. physicochemical characteristics of the phase separation process. *Polymer* **35**:777–785 (1994).
8. P. Giunchedi and U. Conte. Spray-drying as a preparation method of microparticulate drug delivery systems: an overview. *STP Pharma Sci.* **5**:276–290 (1995).
9. S. Shiraishi, T. Imai, and M. Otagiri. Controlled release of indomethacin by chitosan-polyelectrolyte complex: optimization and in vivo/in vitro encapsulation. *J. Control. Rel.* **25**:217–225 (1993).
10. T. L. Whateley. Microcapsules: preparation by interfacial polymerization and interfacial complexation and their application. In S. Benita (ed.), *Microencapsulation: Methods and Industrial Applications*, Vol. 73, Dekker, New York, USA, 1996, pp. 349–375.
11. I. R. D. Santos, J. Richard, B. Pech, C. Thies, and J. P. Benoit. Microencapsulation of protein particles within lipids using a novel supercritical fluid process. *Int. J. Pharm.* **242**:69–78 (2002).
12. F. R. Ahmann, D. L. Citrin, H. A. deHaan, P. Guinan, V. C. Jordan, W. Kreis, M. Scott, and D. L. Trump. Zoladex: a sustained-release, monthly luteinizing hormone-releasing hormone analogue for the treatment of advanced prostate cancer. *J. Clin. Oncol.* **5**:912–917 (1987).
13. D. M. Cook, B. M. Biller, M. L. Vance, A. R. Hoffman, L. S. Phillips, K. M. Ford, D. P. Benziger, A. Illeperuma, S. L. Blethen, K. M. Attie, L. N. Dao, J. D. Reimann, and P. J. Fielder. The pharmacokinetic and pharmacodynamic characteristics of a long-acting growth hormone (GH) preparation (nutropin depot) in GH-deficient adults. *J. Clin. Endocrinol. Metab.* **87**:4508–4514 (2002).
14. I. Lancranjan, C. Bruns, P. Grass, P. Jaquet, J. Jervell, P. Kendall-Taylor, S. W. Lamberts, P. Marbach, H. Orskov, G. Pagani, M. Sheppard, and L. Simionescu. Sandostatin LAR: a promising therapeutic tool in the management of acromegalic patients. *Metabolism* **45**:67–71 (1996).
15. A. M. Dlugi, J. D. Miller, and J. Knittle. Lupron depot (leuprolide acetate for depot suspension) in the treatment of endometriosis: a randomized, placebo-controlled, double-blind study. Lupron Study Group. *Fertil. Steril.* **54**:419–427 (1990).
16. M. van de Weert, W. E. Hennink, and W. Jiskoot. Protein instability in PLGA microparticles. *Pharm. Res.* **17**:1159–1167 (2000).
17. C. Perez, I. J. Castellanos, H. R. Costantino, W. Al-Azzam, and K. Griebenow. Recent trends in stabilizing protein structure upon encapsulation and release from bioerodible polymers. *J. Pharm. Pharmacol.* **54**:301–313 (2002).
18. Y. Yeo and K. Park. Microencapsulation of protein drugs: a novel approach. In D. L. Wise, V. Hasirci, K.-U. Lewandrowski, M. J. Yaszemski, D. E. Altobelli, and D. J. Trantolo (eds.), *Biomaterials Handbook - Advanced Applications of Basic Sciences and Bioengineering*, Marcel Dekker, New York, 2004, pp. 305–332.
19. J. L. Cleland and A. J. S. Jones. Stable formulations of recombinant human growth hormone and interferon-gamma for microencapsulation in biodegradable microspheres. *Pharm. Res.* **13**:1464–1475 (1996).
20. H. Sah. Protein instability toward organic solvent/water emulsification: implications for protein microencapsulation into microspheres. *PDA J. Pharm. Sci. Technol.* **53**:3–10 (1999).
21. W. Lu and T. G. Park. Protein release from poly(lactic-co-glycolic acid) microspheres: protein stability problems. *PDA J. Pharm. Sci. Technol.* **49**:13–19 (1995).
22. T. Uchida, K. Shiosaki, Y. Nakada, K. Fukada, Y. Eda, S. Tokiyoshi, N. Nagareya, and K. Matsuyama. Microencapsulation of hepatitis B core antigen for vaccine preparation. *Pharm. Res.* **15**:1708–1713 (1998).
23. H. K. Kim and T. G. Park. Microencapsulation of human growth hormone within biodegradable polyester microspheres: protein aggregation stability and incomplete release mechanism. *Biotechnol. Bioeng.* **65**:659–667 (1999).
24. M. Iwata, T. Tanaka, Y. Nakamura, and J. W. McGinity. Selection of the solvent system for the preparation of poly(D,L-lactic-co-glycolic acid) microspheres containing tumor necrosis factor-alpha (TNF- α). *Int. J. Pharm.* **160**:145–156 (1998).

25. M. Morlock, H. Koll, G. Winter, and T. Kissel. Microencapsulation of rh-erythropoietin, using biodegradable PLGA: protein stability and the effects of stabilizing excipients. *Eur. J. Pharm. Biopharm.* **43**:29–36 (1997).
26. M. F. Zambaux, F. Bonneaux, R. Gref, E. Dellacherie, and C. Vigneron. Preparation and characterization of protein C-loaded PLA nanoparticles. *J. Control. Rel.* **60**:179–188 (1999).
27. C. Perez and K. Griebenow. Improved activity and stability of lysozyme at the water/methylene chloride interface: enzyme unfolding and aggregation and its prevention by polyols. *J. Pharm. Pharmacol.* **53**:1217–1226 (2001).
28. M. van de Weert, J. Hoehstetter, W. E. Hennink, and D. J. A. Crommelin. The effect of a water/organic solvent interface on the structural stability of lysozyme. *J. Control. Rel.* **68**:351–359 (2000).
29. T. Knubovets, J. J. Osterhout, and A. M. Klibanov. Structure of lysozyme dissolved in neat organic solvents as assessed by NMR and CD spectroscopies. *Biotechnol. Bioeng.* **63**:242–248 (1999).
30. W. Wang. Instability, stabilization, and formulation of liquid protein pharmaceuticals. *Int. J. Pharm.* **185**:129–188 (1999).
31. M. C. Lai and E. M. Topp. Solid-state chemical stability of proteins and peptides. *J. Pharm. Sci.* **88**:489–500 (1999).
32. T. G. Park, H. Y. Lee, and Y. S. Nam. A new preparation method for protein loaded poly(L-lactic-co-glycolic acid) microspheres and protein release mechanism study. *J. Control. Rel.* **55**:181–191 (1998).
33. G. Crotts and T. G. Park. Stability and release of bovine serum albumin encapsulated within PLGA microparticles. *J. Control. Rel.* **44**:123–134 (1997).
34. International Conference on Harmonisation of Technical Requirements for Registration of Pharmaceuticals for Human Use (ICH) guidance for industry Q3C Impurities: Residual Solvents (1997) U.S. Food and Drug Administration, Rockville, MD, USA.
35. M. J. Alonso, R. K. Gupta, C. Min, G. R. Siber, and R. Langer. Biodegradable microspheres as controlled-release tetanus toxoid delivery systems. *Vaccine* **12**:299–306 (1994).
36. D. Blanco and M. J. Alonso. Protein encapsulation and release from poly(lactide-co-glycolide) microspheres: effect of the protein and polymer properties and of the co-encapsulation of surfactants. *Eur. J. Pharm. Biopharm.* **45**:285–294 (1998).
37. T. Freytag, A. Dashevsky, L. Tillman, G. E. Hardee, and R. Bodmeier. Improvement of the encapsulation efficiency of oligonucleotide-containing biodegradable microspheres. *J. Control. Rel.* **69**:197–207 (2000).
38. G. E. Hildebrand and J. W. Tack. Microencapsulation of peptides and proteins. *Int. J. Pharm.* **196**:173–176 (2000).
39. C. Stureson and J. Carlfors. Incorporation of protein in PLG microspheres with retention of bioactivity. *J. Control. Rel.* **67**:171–178 (2000).
40. X. M. Lam, E. T. Duenas, and J. L. Cleland. Encapsulation and stabilization of nerve growth factor into poly(lactic-co-glycolic acid) microspheres. *J. Pharm. Sci.* **90**:1356–1365 (2001).
41. K. S. Soppimath and T. M. Aminabhavi. Ethyl acetate as a dispersing solvent in the production of poly(DL-lactide-co-glycolide) microspheres: effect of process parameters and polymer type. *J. Microencapsulation* **19**:281–292 (2002).
42. M. Reslow, N.-O. Gustafsson, M. Jonsson, and T. Laakso. Polymer coated starch microspheres as protein delivery system, *29th International Symposium on Controlled Release of Bioactive Materials*, Seoul, Korea, 2002, Controlled Release Society, Minneapolis, MN, USA pp. 698.
43. A. N. Martin. *Physical Pharmacy*, Lea & Febiger, Philadelphia, 1993.
44. Y. Yeo, O. A. Basaran, and K. Park. A new process for making reservoir-type microcapsules using ink-jet technology and interfacial phase separation. *J. Control. Rel.* **93**:161–173 (2003).
45. S. Cohen, T. Yoshioka, M. Lucarelli, L. H. Hwang, and R. Langer. Controlled delivery systems for proteins based on PLGA microspheres. *Pharm. Res.* **8**:713–720 (1991).
46. H. Sah. Protein behavior at the water/methylene chloride interface. *J. Pharm. Sci.* **88**:1320–1325 (1999).
47. H. Sah. Connection between interfacial tension kinetics and protein instability at water/organic solvent interface, *28th International Symposium on Controlled Release of Bioactive Materials and 4th Consumer & Diversified Products Conference*, Vol. 2, San Diego, CA, United States, 2001, Controlled Release Society, Minneapolis, MN, USA pp. 954–955.
48. H. Sah. Stabilization of proteins against methylene chloride/water interface-induced denaturation and aggregation. *J. Control. Rel.* **58**:143–151 (1999).
49. H. Sah, S.-K. Choi, H.-G. Choi, and C.-S. Yong. Relation of dynamic changes in interfacial tension to protein destabilization upon emulsification. *Arch. Pharmacol. Res.* **25**:381–386 (2002).
50. C. Berkland, K. Kim, and D. W. Pack. Fabrication of PLG microspheres with precisely controlled and monodisperse size distributions. *J. Control. Rel.* **73**:59–74 (2001).
51. C. Berkland, M. King, A. Cox, K. Kim, and D. W. Pack. Precise control of PLG microsphere size provides enhanced control of drug release rate. *J. Control. Rel.* **82**:137–147 (2002).
52. D. Radulescu, N. Schwade, and D. Wawro. Uniform Paclitaxel-loaded biodegradable microspheres manufactured by Ink-Jet technology, *Winter Symposium and 11th International Symposium on Recent Advances in Drug Delivery Systems*, Salt Lake City, Utah, 2003, Controlled Release Society, Minneapolis, MN, USA pp. 126.
53. A. U. Chen and O. A. Basaran. A new method for significantly reducing drop radius without reducing nozzle radius in drop-on-demand drop production. *Phys. Fluids* **14**:L1–L4 (2002).